21st Australasian Fluid Mechanics Conference
Adelaide, Australia
10-13 December 2018

Large-eddy simulations of decaying turbulence using the stretched-vortex subgrid model with artificial damping

T. W. Mattner

School of Mathematical Sciences
The University of Adelaide, Adelaide, South Australia 5005, Australia

Abstract

The stretched-vortex subgrid model is used in conjunction with a fourth-order finite-difference method and artificial damping to run large-eddy simulations of decaying turbulence. By tuning the strength of the damping and the overlap between the subgrid model cutoff length-scale and the computational grid spacing, it is possible to obtain results that are independent of the grid spacing and consistent with reference simulations using a high-resolution spectral method. Artificial damping is useful for controlling numerical dispersion in large-eddy simulations of turbulent mixing.

Introduction

Turbulent flows are characterised by irregular three-dimensional motion over a wide range of spatial and temporal scales. In a direct numerical simulation of turbulent flow, the entire range of relevant physical scales is resolved on a computational grid. In many applications, including aerodynamic, atmospheric and oceanic flows, for example, the range of scales is so enormous that a direct numerical simulation is not computationally feasible. In a large-eddy simulation (LES), only scales larger than some length-scale Δ are resolved on the computational grid, where Δ is much larger than the smallest physical scale, thereby reducing grid size and computational cost. Usually, Δ is equal to the grid spacing h. A subgrid model is used to account for the effect of subgrid scales on the macroscale flow.

Large-eddy simulations are sensitive to numerical errors. Ghosal [1] shows that truncation errors from standard second to eighth-order centred finite-difference schemes exceed subgrid model terms. Numerical experiments using schemes of different order confirm that large-eddy simulations of turbulent flows are susceptible to error from low-order numerical schemes [3, 2]. The problem is avoided by using numerical schemes with a modified wavenumber that approximates a spectral scheme over as much of the resolved wavenumber range as possible, such as spectral, Padé or specially-tuned finite-difference schemes, provided that numerical errors due to aliasing are also controlled. An alternative is to apply the subgrid model at a scale Δ that is larger than the grid spacing h, while filtering scales smaller than Δ [1, 8]. Ghosal [1] shows that the error from a standard eighth-order centred finite-difference scheme is about an order of magnitude less than the subgrid model terms for an overlap $\Delta/h = 2$. For a fourth-order scheme, the error is mostly less than the subgrid model term, except at high resolved wavenumbers where it is of similar magnitude.

Numerical dispersion is another problem for large-eddy simulations that use low-order low-dissipation numerical schemes. In LES of turbulent mixing, numerical dispersion causes artificial undershoots and overshoots of the scalar field [4]. These scalar excursions are unphysical and are especially problematic in the case of active scalars, such as temperature or density. But it is not just scalar fields that are adversely affected. The group velocity of finite-difference schemes that are used in LES are negative at high wavenumber, and this can result in the flow domain being contaminated by spurious numerical waves [11, 12], especially when there is little physical viscous dissipation, as is usually the case in LES. Numerical dispersion can be controlled by introducing some numerical dissipation or damping [9], but this must be applied with care so as not to interfere with the subgrid model.

The aim of this paper is to determine how much overlap $\Delta/h > 1$ is needed to obtain self-consistent simulations of decaying isotropic turbulence using the stretched-vortex model with a fourth-order staggered finite-difference scheme and artificial damping. Artificial damping is introduced by means of an additional term, similar to that used to control numerical dispersion in computational aeroacoustics [10, 11], controlled by a damping parameter α. It is found that for certain combinations of Δ/h and α, it is possible to obtain results that are independent of the grid spacing h and also consistent with spectral simulations.

Computational model

The simulations in this paper are governed by the filtered Navier–Stokes equations for incompressible flow with an added artificial damping term, which are

$$\frac{\partial \overline{u}_i}{\partial x_i} = 0, \tag{1a}$$

$$\frac{\partial \overline{u}_j}{\partial t} + \frac{\partial \overline{u}_i \overline{u}_j}{\partial x_i} = -\frac{1}{\rho}\frac{\partial \overline{p}}{\partial x_j} + \frac{\partial \overline{\tau}_{ij}}{\partial x_i} - \frac{\partial \tau^{\mathrm{R}}_{ij}}{\partial x_i} - D(\overline{u}_j), \tag{1b}$$

where x_j and u_j are Cartesian components of the Eulerian position and velocity, respectively, p is the pressure, ρ is the density (which is constant), τ_{ij} is the viscous stress tensor,

$$\tau_{ij} = \nu\left(\frac{\partial u_i}{\partial x_j} + \frac{\partial u_j}{\partial x_i}\right)$$

and ν is the kinematic viscosity. The overline denotes macroscale quantities that are solved for in the simulation. The quantity in the second-to-last term of (1b) is the residual-stress tensor,

$$\tau^{\mathrm{R}}_{ij} = \overline{u_i u_j} - \overline{u}_i \overline{u}_j,$$

which accounts for the effects of the unresolved residual quantities on the resolved macroscale flow. The last term in (1b) is the artificial damping term, which is discussed below.

The residual-stress tensor is determined by the stretched-vortex model of Misra & Pullin [6], which is

$$\tau^{\mathrm{R}}_{ij} = K(\delta_{ij} - e^v_i e^v_j), \tag{2}$$

where K is the subgrid kinetic energy and e^v_i are the components of a unit vector that is aligned with the subgrid vortex axis. The subgrid kinetic energy is determined by

$$K = \int_{\kappa_c}^{\infty} E(\kappa)\,\mathrm{d}\kappa, \tag{3}$$

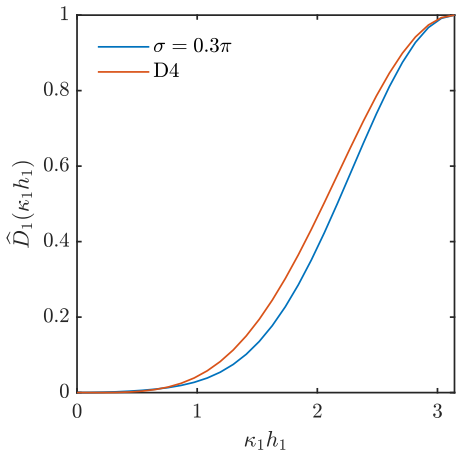

Figure 1: The one-dimensional Fourier transform of the damping function used in this paper (D4), compared with that of the optimised $\sigma = 0.3\pi$ damping function developed by Tam & Shen [10].

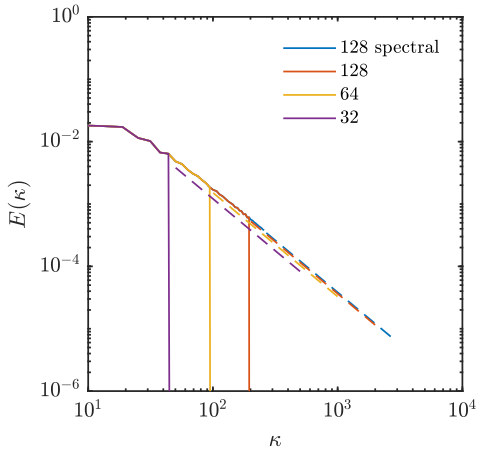

Figure 2: Initial energy spectrum $E(\kappa)$ for the reference spectral simulation (blue) and three grid resolutions with $\Delta/h = 2$ (red, orange, purple). The solid lines are the macroscale spectra and the dashed lines are the subgrid continuation of the spectrum as determined by the model. The cutoff wavenumber κ_c for each grid is indicated by the vertical lines.

where $\kappa = (\kappa_i\kappa_i)^{1/2}$ is the wave-number, $\kappa_c = \pi/\Delta$ is the cutoff wavenumber, $E(\kappa)$ is the spectrum of the Lundgren spiral vortex,

$$E(\kappa) = \mathcal{K}_0\varepsilon^{2/3}\kappa^{-5/3}e^{-\lambda_\nu^2\kappa^2}, \tag{4}$$

$\mathcal{K}_0$ is the Kolmogorov prefactor, ε is the local dissipation rate, $\lambda_\nu^2 = 2\nu/(3|a|)$ and a is the axial strain along the subgrid vortex axis [13]. The group $\mathcal{K}_0\varepsilon^{2/3}$ is calculated from

$$\mathcal{K}_0\varepsilon^{2/3} = \frac{4}{3}\frac{\overline{S}_{ij}\overline{S}_{ij}}{\kappa_c^{4/3}}, \tag{5}$$

instead of the usual second-order structure function [5]. The rate-of-strain parameter a is obtained by assuming that the subgrid dissipation,

$$\varepsilon_{sg} = 2\nu\int_{\kappa_c}^{\infty}\kappa^2 E(\kappa)\,d\kappa, \tag{6}$$

is equal to the transfer of kinetic energy from resolved to subgrid scales, that is,

$$\varepsilon_{sg} = -\overline{S}_{ij}\tau_{ij}^{R} = K\overline{a}, \tag{7}$$

where $\overline{a} = e_i^v e_j^v \overline{S}_{ij}$ is the component of the resolved rate-of-strain tensor along the subgrid vortex axis [5]. Subgrid vortices are assumed to align either with the principal extensional eigenvector of the resolved rate-of-strain tensor, $\overline{S}_{ij}$, or the resolved vorticity vector, $\overline{\omega}$. The respective proportions are λ and $(1-\lambda)$, where

$$\lambda = \frac{\lambda_3}{\lambda_3 + |\overline{\omega}|} \tag{8}$$

and λ_3 is the principal extensional eigenvalue [2].

The governing equations (1) are discretised using fourth-order finite-difference and interpolation operators on a staggered grid [7]. The artificial damping term is

$$D(\overline{u}_j) = \frac{\alpha U_a}{h_i}D_i(\overline{u}_j), \tag{9}$$

where h_i is the grid spacing in the ith direction, α is a damping coefficient, U_a is the characteristic velocity scale of the flow and $D_i(\phi)$ is the operator obtained by applying the interpolation operator twice on ϕ in the ith direction and subtracting the result from ϕ. This damping operator is convenient because the necessary interpolation operators are already available in the numerical implementation, but it is not optimal. Figure 1 shows that this damping operator is a little more dissipative for intermediate wavenumbers than the optimised $\sigma = 0.3\pi$ damping operator developed by Tam & Shen [10].

The simulation domain is a cube with edge length $L = 1$. Simulations are run using grids of size $N = 32$, 64 and 128 with uniform grid spacing $h = 1/N$ and periodic boundary conditions in each coordinate direction. The Reynolds number based on the the characteristic velocity $U_a = 1$ and the edge length of the cube is $\mathrm{Re} = 10^{12}$. At this Reynolds number, there is almost no viscous dissipation by the resolved scales. The explicit low-storage Runge–Kutta scheme recommended by Williamson [14] is used for time stepping. A dealiased Fourier spectral simulation with no artificial damping is used as a reference simulation.

The initial velocity field is a random solenoidal vector field whose energy spectrum is

$$E_0(\kappa) = A\kappa^{-5/3}\left[\frac{\kappa}{\left(\kappa^2 + \frac{5}{6}\kappa_{peak}^2\right)^{1/2}}\right]^{11/3}. \tag{10}$$

The parameter A is chosen so that the initial volume-averaged kinetic energy is unity. The parameter κ_{peak} is the wavenumber at which the energy spectrum is maximum. This is set to a low value of $\kappa_{peak} = 4\pi$ in order to create a reasonable extent of $\kappa^{-5/3}$ for the coarsest grids, as is assumed in the derivation of (5), but this also means that the evolution of the flow is likely to be affected by periodicity. The initial velocity field is generated on a fine 256^3 grid, which is filtered using a sharp-spectral filter to create initial velocity fields for the grids used in the simulations. This ensures that each simulation uses the same initial condition, at least down to scales resolved by the respective grids. Figure 2 shows the initial macroscale and subgrid energy spectra for each of the grids with $\Delta/h = 2$. The agreement between the subgrid and the macroscale spectra near the cutoff wavenumber κ_c for the larger grid sizes verifies that the model estimate of $\mathcal{K}_0\varepsilon^{2/3}$ is accurate when the macroscale spectrum is close to a $\kappa^{-5/3}$ power law.

Results

The total volume-averaged kinetic energy is estimated by

$$\tfrac{1}{2}\langle u_i u_i \rangle \approx \tfrac{1}{2}\langle \overline{u}_i \overline{u}_i \rangle + \langle K \rangle$$

where $\langle \cdot \rangle$ denotes the volume average. The first term on the right hand side is calculated from the macroscale velocity that is resolved on the computational grid, while the second term is calculated from the subgrid model (3).

When a spectral method is used without artifical damping, the total volume-averaged kinetic energy is almost independent of grid size (figure 3a). This verifies that the model correctly increases the subgrid kinetic energy to compensate for the decrease in resolved macroscale kinetic energy as the grid spacing is increased when high-resolution numerical methods are used. There is a 10% discrepancy in the early stages of the $N = 32$ spectral simulation, at which time the subgrid kinetic energy is more than 20% of the total. This is consistent with the poorer estimate of the subgrid spectrum for $N = 32$ in figure 2. Even so, this discrepancy does not persist beyond $t \approx 0.15$.

When the fourth-order finite-difference scheme is used in conjunction with strong damping ($\alpha = 1$) and no overlap ($\Delta/h = 1$), the total volume-averaged kinetic energy is grid dependent and different to that of the reference spectral simulation (figure 3b). However, when more moderate values of the damping coefficient are used in conjunction with some overlap, it is possible to obtain results that are less dependent on grid resolution and more consistent with simulations using spectral methods. Figures 3(b) and 3(c) show that this is the case for the combinations $\alpha = 0.1$ with $\Delta/h = 1.6$ and $\alpha = 0.3$ with $\Delta/h = 2$ when $N = 64$ and 128. There is a discrepancy of up to 20% of the total volume-averaged kinetic energy in the initial stages of the $N = 32$ simulations, subsequently decreasing to less than 10% as the flow evolves. Once again, the discrepancy occurs when the subgrid kinetic energy is more than 20% of the total.

In the spectral simulations, there is evidence of some attenuation of the macroscale spectrum at high resolved wavenumbers in the form of a departure from a $\kappa^{-5/3}$ spectrum (figure 4a). However, this is mild when compared with the attenuation for $\alpha = 0.3$ with $\Delta/h = 2$ (figure 4b), which is due to the combined action of artificial damping and enhanced subgrid dissipation for $\Delta/h > 1$. Figure 4(b) shows that there is a substantial jump between the resolved macroscale spectra and the subgrid extensions for $\alpha = 0.3$ with $\Delta/h = 2$. Despite this, the subgrid spectra are only weakly dependent on the grid resolution. This is also true for the combination $\alpha = 0.1$ with $\Delta/h = 1.6$, which is not shown, but not all other combinations. There is a noticeable difference between the subgrid spectra for $\alpha = 0.3$ with $\Delta/h = 2$ and those of the spectral simulation. This is not unexpected, because the formula for $\mathcal{K}_0\varepsilon^{2/3}$ (5), which determines the magnitude of the subgrid spectrum, assumes that the macroscale spectrum follows a $\kappa^{-5/3}$ power law near the model cutoff κ_c, and that the cutoff at that wavenumber is sharp, which is certainly not true for simulations with artificial damping and overlap.

It is possible to estimate the contributions of the subgrid model and the artificial damping term to the rate of dissipation of macroscale kinetic energy by calculating the volume average of (7) and estimating the time derivative of $\frac{1}{2}\langle \overline{u}_i \overline{u}_i \rangle$, respectively. For $\alpha = 0.1$ with $\Delta/h = 1.6$, the subgrid model accounts for about 70% of the macroscale kinetic energy dissipation. For $\alpha = 0.3$ with $\Delta/h = 2$, the subgrid model accounts for about 60% of the dissipation.

Conclusions

Self-consistent simulations of decaying turbulence using the stretched-vortex model with a fourth-order finite-difference scheme and artificial damping are possible by appropriate choice of overlap Δ/h and damping parameter α. However, the simple damping operator used in this paper substantially alters the macroscale spectrum and accounts for a significant fraction of the macroscale kinetic energy dissipation.

*

References

[1] Ghosal, S., An analysis of numerical errors in large-eddy simulations of turbulence, *Journal of Computational Physics*, **125**, 1996, 187–206.

[2] Kosović, B., Pullin, D. I. and Samtaney, R., Subgrid-scale modeling for large-eddy simulations of compressible turbulence, *Physics of Fluids*, **14**, 2002, 1511–1522.

[3] Kravchenko, A. G. and Moin, P., On the Effect of Numerical Errors in Large Eddy Simulations of Turbulent Flows, *Journal of Computational Physics*, **131**, 1997, 310–322.

[4] Matheou, G. and Dimotakis, P. E., Scalar excursions in large-eddy simulations, *Journal of Computational Physics*, **327**, 2016, 97–120.

[5] Mattner, T. W., A refined stretched-vortex model for large-eddy simulation of turbulent mixing layers, in *17th Australasian Fluid Mechanics Conference*, 2010.

[6] Misra, A. and Pullin, D. I., A vortex-based subgrid stress model for large-eddy simulation, *Physics of Fluids*, **9**, 1997, 2443–2454.

[7] Morinishi, Y., Lund, T. S., Vasilyev, O. V. and Moin, P., Fully Conservative Higher Order Finite Difference Schemes for Incompressible Flow, *Journal of Computational Physics*, **143**, 1998, 90–124.

[8] Pope, S. B., Ten questions concerning the large-eddy simulation of turbulent flows, *New J. Phys.*, **6**, 2004, 35.

[9] Sharan, N., Matheou, G. and Dimotakis, P. E., Mixing, scalar boundedness, and numerical dissipation in large-eddy simulations, *Journal of Computational Physics*, **369**, 2018, 148–172.

[10] Tam, C. and Shen, H., Direct computation of nonlinear acoustic pulses using high-order finite difference schemes, American Institute of Aeronautics and Astronautics, 1993.

[11] Tam, C. K. W., Computational aeroacoustics - Issues and methods, *AIAA Journal*, **33**, 1995, 1788–1796.

[12] Trefethen, L., Group Velocity in Finite Difference Schemes, *SIAM Rev.*, **24**, 1982, 113–136.

[13] Voelkl, T., Pullin, D. I. and Chan, D. C., A physical-space version of the stretched-vortex subgrid-stress model for large-eddy simulation, *Physics of Fluids*, **12**, 2000, 1810–1825.

[14] Williamson, J. H., Low-storage Runge-Kutta schemes, *Journal of Computational Physics*, **35**, 1980, 48–56.

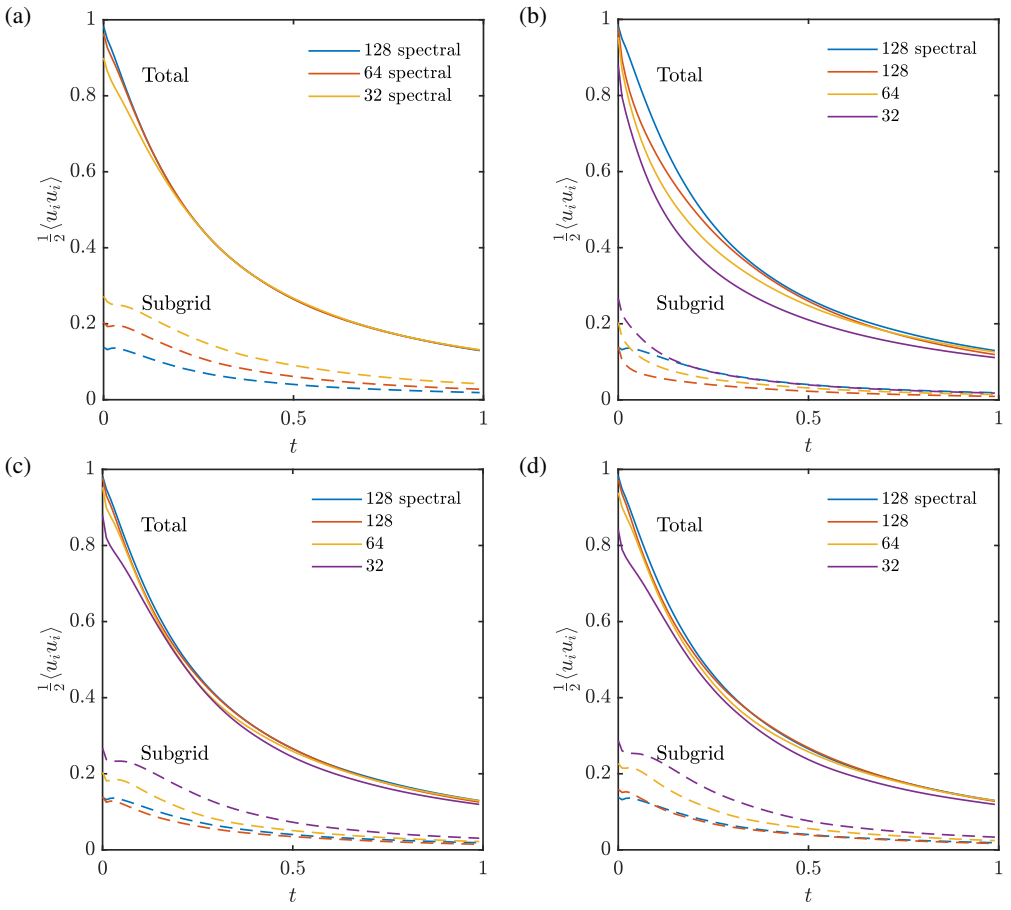

Figure 3: Turbulent kinetic energy $\frac{1}{2}\langle u_i u_i \rangle$ versus time t for (a) reference spectral simulation, (b) $\alpha = 1$, $\Delta/h = 1.6$, (c) $\alpha = 0.1$, $\Delta/h = 1.6$ and (d) $\alpha = 0.3$, $\Delta/h = 2$ at three grid resolutions, as indicated in the legend. The solid lines are the total turbulent kinetic energy, which is the sum of the resolved and subgrid kinetic energy. The dashed lines are the subgrid kinetic energy.

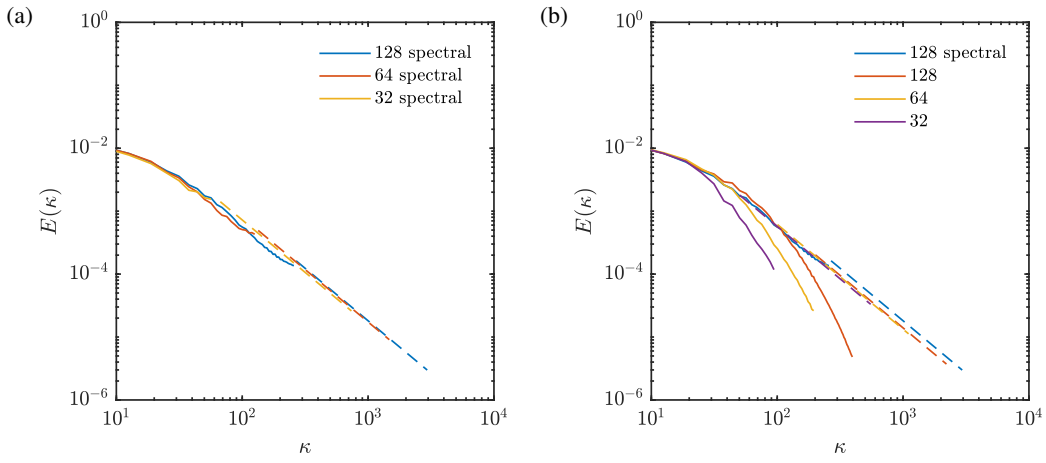

Figure 4: Energy spectra $E(\kappa)$ at $t = 0.3$ for (a) reference spectral simulation and (b) $\alpha = 0.3$, $\Delta/h = 2$ at three grid resolutions, as indicated in the legend. The solid lines are the resolved macroscale spectra and the dashed lines are the subgrid spectra, as determined by the subgrid model. The subgrid spectra commence from the model cutoff wavenumber $\kappa > \kappa_c = \pi/\Delta$, while the macroscale spectra continue to the maximum grid wavenumber $\kappa < \kappa_{\max} = \pi/h$, so there is some overlap.